

Human GUCY2C-Targeted Chimeric Antigen Receptor (CAR)-Expressing T Cells Eliminate Colorectal Cancer Metastases



Michael S. Magee^{1,2}, Tara S. Abraham², Trevor R. Baybutt², John C. Flickinger Jr², Natalie A. Ridge², Glen P. Marszalowicz³, Priyanka Prajapati², Adam R. Hersperger⁴, Scott A. Waldman², and Adam E. Snook²

Abstract

One major hurdle to the success of adoptive T-cell therapy is the identification of antigens that permit effective targeting of tumors in the absence of toxicities to essential organs. Previous work has demonstrated that T cells engineered to express chimeric antigen receptors (CAR-T cells) targeting the murine homolog of the colorectal cancer antigen GUCY2C treat established colorectal cancer metastases, without toxicity to the normal GUCY2C-expressing intestinal epithelium, reflecting structural compartmentalization of endogenous GUCY2C to apical membranes comprising the intestinal lumen. Here, we examined the utility of a human-specific, GUCY2C-directed single-chain variable fragment as the basis for a CAR construct targeting human GUCY2C-expressing metastases. Human GUCY2C-targeted murine

CAR-T cells promoted antigen-dependent T-cell activation quantified by activation marker upregulation, cytokine production, and killing of GUCY2C-expressing, but not GUCY2C-deficient, cancer cells *in vitro*. GUCY2C CAR-T cells provided long-term protection against lung metastases of murine colorectal cancer cells engineered to express human GUCY2C in a syngeneic mouse model. GUCY2C murine CAR-T cells recognized and killed human colorectal cancer cells endogenously expressing GUCY2C, providing durable survival in a human xenograft model in immunodeficient mice. Thus, we have identified a human GUCY2C-specific CAR-T cell therapy approach that may be developed for the treatment of GUCY2C-expressing metastatic colorectal cancer. *Cancer Immunol Res*; 6(5): 509–16. ©2018 AACR.

Introduction

Chimeric antigen receptor (CAR)-expressing T cells are effective in patients with advanced B-cell malignancies and neuroblastoma (1–3). However, the clinical utility of adoptively transferred T cells has been limited in patients with colorectal cancer, reflecting antigen "on-target, off-tumor" toxicities limiting treatment options (4, 5). Guanylyl cyclase C (GUCY2C) is a membrane-bound receptor that produces the second messenger cGMP following activation by its hormone ligands guanylin or uroguanylin, regulating intestinal homeostasis, tumorigenesis, and obesity (6). GUCY2C cell surface expression is confined to luminal surfaces of the intestinal epithelium and a subset of hypothalamic neurons (7). Its expression is maintained in >95% of colorectal cancer metastases, and it is ectopically expressed in tumors that evolve from intestinal

metaplasia, including esophageal, gastric, and pancreatic cancers (8, 9). The inaccessibility of GUCY2C in the apical membranes of polarized epithelial tissue (10), due to subcellular restriction of GUCY2C, creates a therapeutic opportunity to target metastatic lesions of colorectal origin that have lost apical–basolateral polarization (11), without concomitant intestinal toxicity. Previously, we demonstrated in a syngeneic, immunocompetent mouse model that CAR-T cells targeting murine GUCY2C were effective against colorectal cancer metastatic to lung in the absence of intestinal toxicities (12). Similarly, other GUCY2C-targeted therapeutics, including antibody–drug conjugates (13) and vaccines (14, 15), are safe in preclinical animal models, and therapeutic regimens utilizing these platforms are in clinical trials for metastatic esophageal, gastric, pancreatic, and colorectal cancers (NCT02202759, NCT02202785, and NCT01972737). The safety of these therapeutic regimens, in the context of GUCY2C expression across the rostral–caudal axis of intestine, reflects compartmentalized expression of GUCY2C, enriched in apical, but limited in basolateral, membranes of epithelial cells (16–19). Systemic radiolabeled imaging agents conjugated to GUCY2C ligand target GUCY2C-expressing metastases without localizing in intestine (10), confirming the mucosal compartmentalization of the receptor. Tumors express up to 10-fold greater amounts of GUCY2C, compared with normal epithelial cells (9, 20), potentially creating a quantitative therapeutic window to discriminate receptor overexpressing tumors from intestinal epithelium (21) with low/absent GUCY2C in basolateral membranes (19).

¹Bluebird Bio, Cambridge, Massachusetts. ²Department of Pharmacology and Experimental Therapeutics, Thomas Jefferson University, Philadelphia, Pennsylvania. ³School of Biomedical Engineering, Science and Health Systems, Drexel University, Philadelphia, Pennsylvania. ⁴Department of Microbiology and Immunology, Thomas Jefferson University, Philadelphia, Pennsylvania.

Note: Supplementary data for this article are available at Cancer Immunology Research Online (<http://cancerimmunolres.aacrjournals.org/>).

Corresponding Author: Adam E. Snook, Thomas Jefferson University, 1020 Locust Street, JAH 368E, Philadelphia, PA 19107. Phone: 215-503-7445; Fax: 215-955-7006; E-mail: adam.snook@jefferson.edu

doi: 10.1158/2326-6066.CIR-16-0362

©2018 American Association for Cancer Research.

Here, we identified a human GUCY2C-targeted CAR that could potentially be used in patients with GUCY2C-expressing gastrointestinal malignancies. This CAR induced antigen-dependent T-cell activation, cytokine production, and cytolytic activity. Human GUCY2C-targeted CAR-T cells were effective against metastatic tumors in immunocompetent, syngeneic mouse models, as well as xenograft models of human colorectal cancer.

Materials and Methods

Cell lines and reagents

CT26 and β -galactosidase-expressing CT26.CL25 mouse colorectal cancer cell lines and the human colorectal cancer cell lines T84 and SW480 were obtained from ATCC, and large stocks of low-passage cells were cryopreserved. Cells were authenticated by the original suppliers and routinely authenticated by morphology, growth, antibiotic resistance (where appropriate), appropriate GUCY2C and β -galactosidase expression, and pattern of metastasis *in vivo* and routinely screened for *mycoplasma* using the Universal Mycoplasma Detection Kit (ATCC, Cat. No. 30-1012K). Before injection into mice, cells were routinely cultured for <2 weeks. The gene encoding human GUCY2C was codon-optimized (Supplementary Fig. S1) and synthesized (Gene Art, Life Technologies) and cloned into the retroviral construct pMSCVpuro (Clontech). CT26.hGUCY2C and CT26.CL25.hGUCY2C were generated by transducing CT26 and CT26.CL25 cells with retroviral supernatants encoding hGUCY2C, followed by selection with puromycin. Retroviral supernatants were produced by transfecting the Phoenix-Eco retroviral packaging cell line (Gary Nolan, Stanford University) with pMSCV-Puro (Clontech) or hGUCY2C-pMSCV-Puro and the pCL-Eco (Imgenex) retroviral packaging vector (12). Luciferase-containing T84.fluc cells were generated by transduction with lentiviral supernatants generated by transfecting 293FT cells (Invitrogen) with pLenti4-V5-GW-luciferase.puro (kindly provided by Andrew Aplin, Thomas Jefferson University) and the ViraPower Lentiviral Packaging Mix (Invitrogen) according to the manufacturer's instructions, followed by selection in puromycin. The single-chain variable fragment (scFv) from the human GUCY2C-specific antibody 5F9 (Supplementary Fig. S2) was cloned into the pFUSE-rlgG-Fc2 (IL2ss) plasmid (Invivogen), producing a 5F9 scFv fusion protein with rabbit Fc (5F9-rFc). 5F9-rFc was collected in supernatants of transfected 293F cells (Life Technologies), titrated in ELISA plates (Nunc-Immuno PolySorp) coated with BSA or recombinant 6xHis-tagged hGUCY2C extracellular domain (6xHis-hGUCY2C_{ECD}) protein purified under contract from HEK293-6E cells by GenScript and detected with HRP-conjugated goat anti-rabbit (Jackson ImmunoResearch). For flow cytometry, cells were stained with 5F9-rFc or control supernatants from untransfected 293F cells diluted in FACS buffer (1% heat-inactivated FBS in PBS), followed by secondary Alexa Fluor 488-conjugated anti-rabbit (Life Technologies) in FACS buffer. Cells were fixed with 2% paraformaldehyde (PFA; Affymetrix) and analyzed using the BD LSR II flow cytometer and FlowJo v10 software (TreeStar).

Murine CAR-T cell generation

Murine CAR components were used to produce a third-generation, codon-optimized retroviral CAR construct as previously described (12). A codon-optimized scFv sequence derived from

the 5F9 human GUCY2C-specific antibody (Supplementary Fig. S2) was cloned into a CAR construct containing murine sequences of the BiP signal peptide, CD8 α hinge region, CD28 transmembrane and intracellular domains, and 4-1BB (CD137) and CD3 ζ intracellular domains, producing the 5F9.m28BBz CAR construct (Supplementary Fig. S3). CARs derived from the human ERBB2 (Her2)-specific antibody 4D5 or mouse CD19-specific antibody 1D3 (Supplementary Fig. S2) were used as controls as indicated (Control m28BBz). CARs were subcloned into the pMSCV-IRES-GFP (pMIG) retroviral vector (Addgene # 27490). The Phoenix-Eco retroviral packaging cell line (Gary Nolan, Stanford University) was transfected with CAR-pMIG vectors and the pCL-Eco retroviral packaging vector (Imgenex) using the Calcium Phosphate Profection Mammalian Transfection System (Promega). Retrovirus-containing supernatants were collected 48 hours later, filtered through 0.45 μ m filters, and aliquots were frozen at -80°C .

Murine CD8⁺ T cells were negatively selected from BALB/c splenocytes using the CD8 α ⁺ T-cell Isolation Kit II and LS magnetic columns (Miltenyi Biotec). CD8⁺ T cells were subsequently stimulated with anti-CD3/anti-CD28-coated beads (T Cell Activation/Expansion Kit, Miltenyi Biotec) at a 1:1 bead:cell ratio at 1×10^6 cells/mL in cRPMI with recombinant human IL2 (100 U/mL; NCI Repository). The day following stimulation, half of the culture media were carefully replaced with an equal volume of thawed retroviral supernatant in the presence of polybrene (8 μ g/mL; Millipore). Spinoculation was performed at room temperature for 90 minutes at 2,500 rpm followed by incubation at 37°C for 2.5 hours, at which point cells were pelleted and resuspended in fresh media containing IL2 (100 U/mL). T cells were expanded for 7 to 10 days by daily dilution to 1×10^6 cells/mL with fresh cRPMI and IL2, at which point they were used for functional assays.

Human CAR-T cell generation

For studies with human T cells, PBMCs were collected from consenting volunteers in accordance with regulatory and institutional requirements. MACS (STEMCELL Technologies) purified CD8⁺ T cells were negatively selected from individual normal healthy donor whole blood at >90% purity. CAR domains using human sequences were used to produce a third-generation, codon-optimized retroviral CAR construct containing the 5F9 human GUCY2C-specific scFv and human sequences of the GM-CSF signal peptide, CD8 α hinge region, CD28 transmembrane and intracellular domains, and 4-1BB (CD137) and CD3 ζ intracellular domains producing 5F9.h28BBz (Supplementary Fig. S4). CAR-encoding amphotropic γ -retrovirus production was similar to that with murine T cells, but replaced pCL-Eco with the pCL-Ampho packaging plasmid (Imgenex). Retroviral transduction occurred on day 3 or 4 after activation with ImmunoCult CD3/CD28 Activator (STEMCELL Technologies). Cells underwent flow sorting for GFP enrichment on day 7, followed by experimental use on day 10. Throughout the duration in culture, human CD8⁺ T cells were maintained in ImmunoCult-XF media (STEMCELL Technologies) supplemented with 100 U/mL recombinant, human IL2 (NCI Repository).

CAR surface detection

CAR-transduced T cells were stained with the LIVE/DEAD Fixable Aqua Dead Cell Stain Kit (Invitrogen) in PBS, labeled with varying concentrations of 6xHis-hGUCY2C_{ECD} for 1 hour in

PBS 0.5% BSA, stained with anti-5xHis–Alexa Fluor 647 conjugate (Qiagen) and anti-CD8b–PE (clone H35.17.2, BD Biosciences) for 1 hour in PBS 0.5% BSA, fixed with 2% PFA, and analyzed using the BD LSR II flow cytometer and FlowJo software v10 (TreeStar). hGUCY2C binding was determined by mean fluorescence intensity of Alexa Fluor 647 on live CD8⁺ CAR⁺ (GFP⁺) cells. Nonlinear regression analysis (GraphPad Prism v6) was used to determine the K_{av} and B_{max} of GUCY2C–CAR binding.

Mouse T-cell phenotyping, activation markers, and intracellular cytokine staining

For phenotyping, 1×10^6 nontransduced or CAR-transduced mouse T cells were stained with the LIVE/DEAD Fixable Aqua Dead Cell Stain Kit (Invitrogen) in PBS and subsequently stained for surface markers using anti-CD8 α –BV570 (clone RPA-T8; BioLegend), anti-CD45RA–PerCP–Cy5.5 (clone 14.8; BD Biosciences), and anti-CD62L–PE–Cy7 (clone MEL-14; BD Biosciences) for 30 minutes in PBS 0.5% BSA. Cells were subsequently fixed and permeabilized (BD Cytofix/Cytoperm Kit; BD Biosciences) with Cytofix/Cytoperm buffer for 20 minutes at 4°C and stained for intracellular GFP (anti-GFP–Alexa Fluor 488; Invitrogen) for 45 minutes in Perm/Wash buffer to identify CAR-transduced cells. The following subsets were then quantified based on CD45RA and CD62L staining: $T_{n/scm}$ (naïve or T memory stem cells; CD62L⁺CD45RA⁺), T_{cm} (central memory T cells; CD62L⁺CD45RA⁻), T_{em} (effector memory T cells; CD62L⁻CD45RA⁻), and T_{emra} (effector memory T cells expressing CD45RA; CD62L⁻CD45RA⁺).

For activation marker and cytokine analysis, 1×10^6 CAR-transduced mouse T cells were stimulated for 6 hours in tissue culture plates previously coated with 1 μ g/mL GUCY2C in PBS overnight at 4°C or in tissue culture plates containing 1×10^6 CT26 or CT26.hGUCY2C cells. As a positive control, CAR-T cells were incubated for 6 hours with 1 \times Cell Stimulation Cocktail (PMA/Ionomycin, eBioscience). Incubation included 1 \times Protein Transport Inhibitor Cocktail (eBioscience) when assessing intracellular cytokines. Cells were stained with the LIVE/DEAD Fixable Aqua Dead Cell Stain Kit (Invitrogen) and subsequently stained for surface markers using anti-CD8 α –PerCP–Cy5.5 (clone 53.6-7; BD Biosciences), anti-CD69–PE (clone H1.2F3; BD Biosciences), anti-CD25–PE (clone PC61.5, eBioscience), and anti-CD44–APC (clone IM7; BioLegend). Intracellular cytokine staining was performed using the BD Cytofix/Cytoperm Kit (BD Biosciences) and staining with anti-GFP–Alexa488 (Invitrogen), anti-IFN γ –APC–Cy7 (clone XMG1.2; BD Biosciences), anti-TNF α –PE–Cy7 (clone MP6-XT22; BD Biosciences), anti-IL2–APC (clone JES6-5H4; BD Biosciences) and α MIP1 α –PE (clone 39624; R&D Systems). Cells were fixed in 2% PFA and analyzed on a BD LSR II flow cytometer. Analyses were performed using FlowJo v10 software (TreeStar).

Human T-cell activation marker and intracellular cytokine staining

For activation marker and cytokine analysis, 1×10^6 human GUCY2C-directed CAR-transduced human T cells were stimulated for 6 hours in tissue culture plates coated overnight at 4°C with 10 μ g/mL human GUCY2C or BSA control antigen in PBS or with 1 \times Cell Stimulation Cocktail (PMA/Ionomycin, eBioscience) added at the time of plating CAR-T cells. All conditions included 1 \times Protein Transport Inhibitor Cocktail (eBioscience) at the beginning of the incubation period. Cells were stained with the LIVE/DEAD Fixable Aqua Dead Cell

Stain Kit (Invitrogen) in PBS for 10 minutes and subsequently stained for surface markers using anti-CD8–Qdot 800 (clone 3B5, Invitrogen) and anti-CD69–APC (clone L78, BD Biosciences) in PBS 0.5% BSA for 25 minutes. Intracellular cytokine staining was performed using the BD Cytofix/Cytoperm Kit (BD Biosciences) consisting of fixation with Cytofix/Cytoperm buffer for 20 minutes and staining with anti-GFP–Alexa Fluor 488 (Invitrogen), anti-IFN γ –BV605 (clone 4S.B3; BioLegend), anti-TNF α –PerCP–Cy5.5 (clone Mab11; BD Biosciences), and anti-IL2–PE (clone MQ1-17H12; BD Biosciences) in BD perm wash buffer for 45 minutes. Cells were fixed in 2% PFA and analyzed on a BD LSR II flow cytometer. Analyses were performed using FlowJo v10 software (TreeStar).

T-cell cytotoxicity assays

The xCELLigence real-time, cell-mediated cytotoxicity system (Acea Biosciences Inc.) was utilized for assessment of CAR-T cell-mediated cytotoxicity as previously described (12). Briefly, 1×10^4 CT26 or CT26.hGUCY2C or 2.5×10^4 T84 or SW480 cancer cell targets were plated in 150 μ L of growth medium in each well of an E-Plate 16 (Acea Biosciences) and grown overnight in a 37°C incubator, quantifying electrical impedance every 15 minutes using the RTCA DP Analyzer system and RTCA software version 2.0 (Acea Biosciences Inc.). Approximately 24 hours later for mouse and 6 hours for human T-cell experiments, 50 μ L of CAR-T cells were added (5:1 E:T ratio for mouse T cells or 10:1 E:T ratio for human T cells), or 50 μ L of media or 10% Triton-X 100 (Fisher) was added for a final (v/v) of 2.5% Triton-X 100 as negative and positive controls, respectively. Cell-mediated killing was quantified over the next 10 to 20 hours, reading electrical impedance every 15 minutes. Percent specific lysis values were calculated using GraphPad Prism Software v6 for each replicate at each time point, using impedance values following the addition of media and Triton-X 100 for normalization (0% and 100% specific lysis, respectively).

Alternatively, the β -gal release T-cell cytotoxicity assay utilized CT26 cancer cell targets expressing β -galactosidase (CT26.CL25). Cancer cell targets were plated at 2×10^5 cells/well in a 96-well plate and incubated with increasing effector CAR-T cell to cancer cell target ratios for 4 hours at 37°C. Released β -galactosidase was measured in the media using the Galacto-Light Plus System (Applied Biosystems). Maximum release was determined from supernatants of cells that were lysed with supplied lysis buffer. % specific lysis = [(experimental release – spontaneous release)/(maximum release – spontaneous release)] \times 100.

Metastatic tumor models

BALB/c mice and NSG (NOD-*scid* IL2R γ^{null}) mice were obtained from the NCI Animal Production Program and The Jackson Laboratory, respectively. Animal protocols were approved by the Thomas Jefferson University Institutional Animal Care and Use Committee. In syngeneic mouse models, BALB/c mice were injected with 5×10^5 CT26.hGUCY2C cells in 100 μ L of PBS by tail-vein injection to establish lung metastases. On indicated days, mice received a nonmyeloablative dose of 5 Gy total body irradiation in a PanTak, 310 keV X-ray machine (12). Mice received the indicated dose of CAR-T cells produced from CD8⁺ BALB/c T cells in 100 μ L of PBS by tail vein at the indicated time points. Mice were followed for survival or sacrificed on day 18 after cancer cell injection and lungs were stained with India Ink and fixed in Fekete's solution for tumor enumeration (22).

For rechallenge experiments, naïve mice or mice cleared of established tumors by CAR-T cells (referred to as "surviving mice") received one dose of 5×10^5 CT26 or CT26.hGUCY2C via tail-vein injection. Surviving mice were initially challenged 16 to 40 weeks prior to the rechallenge experiment.

In human tumor xenograft models, NSG (23) mice (JAX stock #005557) were injected with 2.5×10^6 T84.fLuc cells in 100 μ L PBS via intraperitoneal injection. Mice received a dose of 10^7 total (not sorted on CAR⁺) T cells produced from CD8⁺ BALB/c T cells in 100 μ L PBS via intraperitoneal injection on day 14 after cancer cell inoculation. Tumor growth was monitored weekly by subcutaneous injection of a 250 μ L solution of 15 mg/mL D-luciferin potassium salt (Gold Biotechnologies) in PBS and imaging

after 8 minutes of exposure using the Caliper IVIS Lumina-XR imaging station (Perkin Elmer). Total radiance (photons/second) was quantified using Living Image In Vivo Imaging Software (Perkin Elmer).

Results and Discussion

hGUCY2C CAR-T cells

A recombinant antibody (clone 5F9) specific for human GUCY2C (hGUCY2C) bound to purified hGUCY2C extracellular domain (Fig. 1A) and murine CT26 colorectal cancer cells engineered to express hGUCY2C, but not hGUCY2C-deficient CT26 cancer cells (Fig. 1B). The 5F9 scFv was used to generate

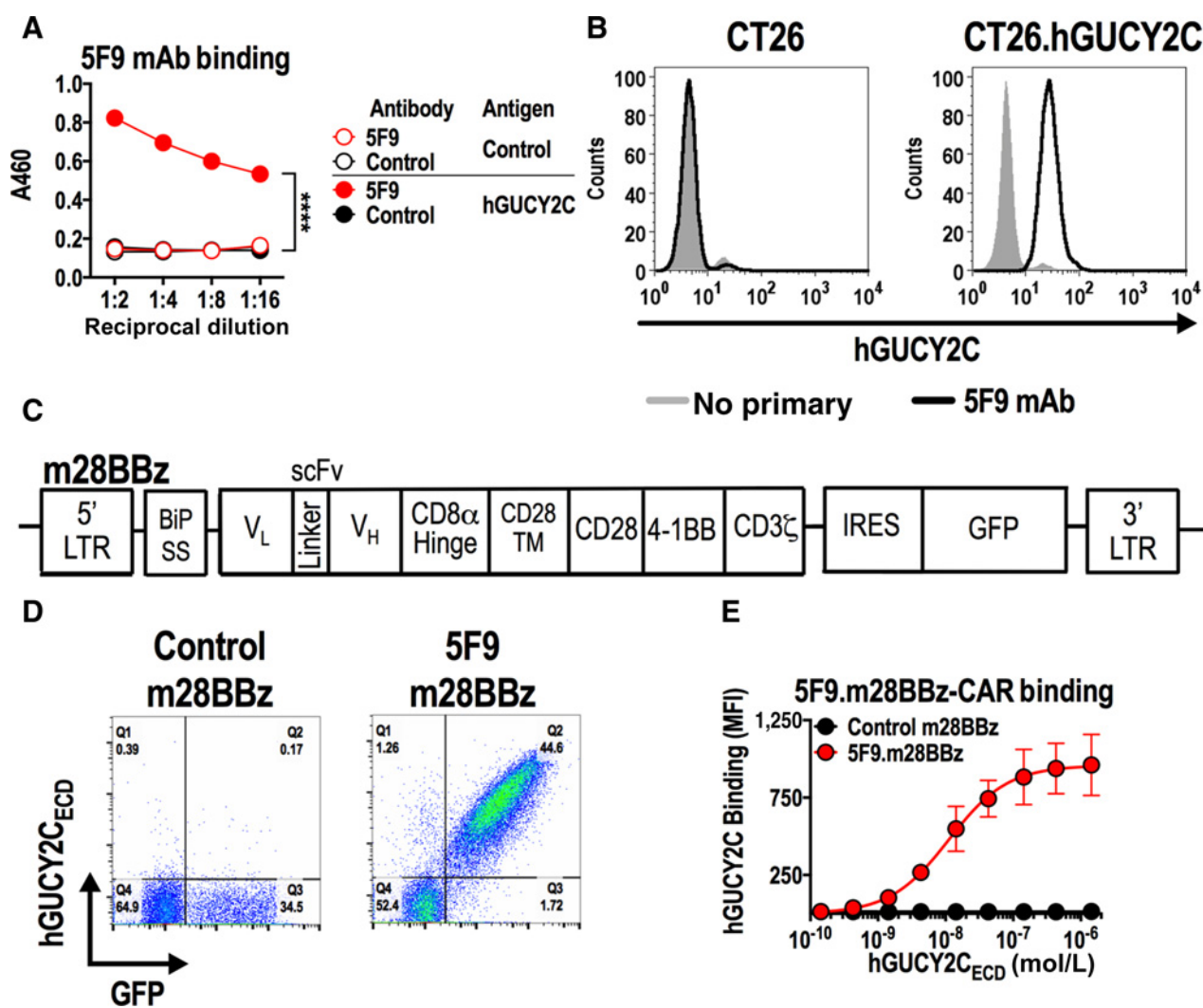


Figure 1.

Generation of human GUCY2C-specific CAR-T cells. **A**, Recombinant 5F9 antibody was assessed by ELISA for specific binding to hGUCY2C_{ECD} or BSA (negative control) plated at 1 μ g/mL. Two-way ANOVA; ****, $P < 0.0001$. **B**, Flow cytometry analysis was performed on parental CT26 mouse colorectal cancer cells or CT26 cells engineered to express hGUCY2C (CT26.hGUCY2C) and stained with 5F9 antibody. **C**, Schematic of the third-generation murine CAR construct containing murine sequences of the BiP signal sequence, 5F9 scFv, CD8 α hinge region, the transmembrane and intracellular domain of CD28, the intracellular domain of 4-1BB (CD137), and the intracellular domain of CD3 ζ (5F9.m28BBz). The CAR construct was inserted into the MSCV retroviral plasmid pMIG upstream of an IRES-GFP marker. **D**, Murine CD8⁺ T cells transduced with a retrovirus containing a control (ID3.m28BBz) CAR or CAR derived from the 5F9 antibody (5F9.m28BBz) were labeled with purified 6xHis-hGUCY2C_{ECD} (10 μ g/mL), detected with anti-5xHis-Alexa Fluor 647 conjugate. Flow plots were gated on live CD8⁺ cells. **E**, 6xHis-hGUCY2C_{ECD} binding curves for 5F9-derived or control (ID3) CARs, gated on live CD8⁺GFP⁺ cells (Supplementary Fig. S5). Combined from 3 independent experiments.

a third-generation murine CAR construct (5F9.m28BBz) containing the BiP signal sequence, CD8 α hinge region, and intracellular CD28, 4-1BB, and CD3 ζ signaling moieties and inserted into a retroviral construct (Fig. 1C). Retroviruses encoding control m28BBz or 5F9.m28BBz CARs were used to transduce murine T cells with ~35% to 45% transduction efficiency, quantified by a GFP transduction marker (Fig. 1D). hGUCY2C-binding avidity (K_{av} = 11.2 nmol/L) and CAR expression (B_{max} = 957.8 MFI), quantified by incubating CAR-T cells with increasing concentrations of purified 6xHis-tagged hGUCY2C_{ECD} followed by detection with labeled α 5xHis antibody and assessment by flow cytometry, was comparable with CARs that exhibited functional reactivity to mouse GUCY2C (ref. 12; Fig. 1D and E; Supplementary Fig. S5).

hGUCY2C CAR mediates T-cell activation and effector function

Transduction of purified mouse CD8⁺ T cells with control m28BBz or hGUCY2C-specific 5F9.m28BBz CAR constructs had no impact on T-cell phenotype compared with non-transduced cells (Fig. 2B), producing a mixture of memory and effector phenotypes [T_{n/scm} (CD62L⁺CD45RA⁺), T_{cm} (CD62L⁺CD45RA⁻), T_{em} (CD62L⁻CD45RA⁻), and T_{emra} (CD62L⁻CD45RA⁺)] similar to other CAR constructs in

CAR-T cells produced in the presence of IL2 (24). hGUCY2C-specific, but not control, CAR-T cells upregulated the activation markers CD25, CD69, and CD44 (Fig. 2C) and produced the effector cytokines IFN γ , TNF α , IL2, and MIP1 α (Fig. 2D) when stimulated with immobilized hGUCY2C_{ECD} protein or CT26. hGUCY2C cells (Supplementary Figs. S6 and S7). Activation marker and cytokine responses were absent when 5F9.m28BBz CAR-T cells were stimulated with BSA or hGUCY2C-deficient CT26 cells, confirming that T-cell activation by the 5F9.m28BBz CAR is antigen-dependent (Fig. 2C and D; Supplementary Figs. S6 and S7). Although 5F9.m28BBz CAR-T cells were inactive against hGUCY2C-deficient CT26 cells *in vitro* (Fig. 2E), they exhibited time-dependent killing of CT26.hGUCY2C cells, quantified using an electrical impedance assay (Fig. 2E) and confirmed in a β -galactosidase release T-cell cytotoxicity assay (Supplementary Fig. S8).

hGUCY2C CAR-T cells oppose metastatic colorectal cancer

The endogenous immune system can induce immunosuppression in the tumor microenvironment and compete with adoptively transferred T cells for resources necessary for long-term persistence (25). In that context, lymphodepletive conditioning regimens, such as low-dose total body irradiation (TBI)

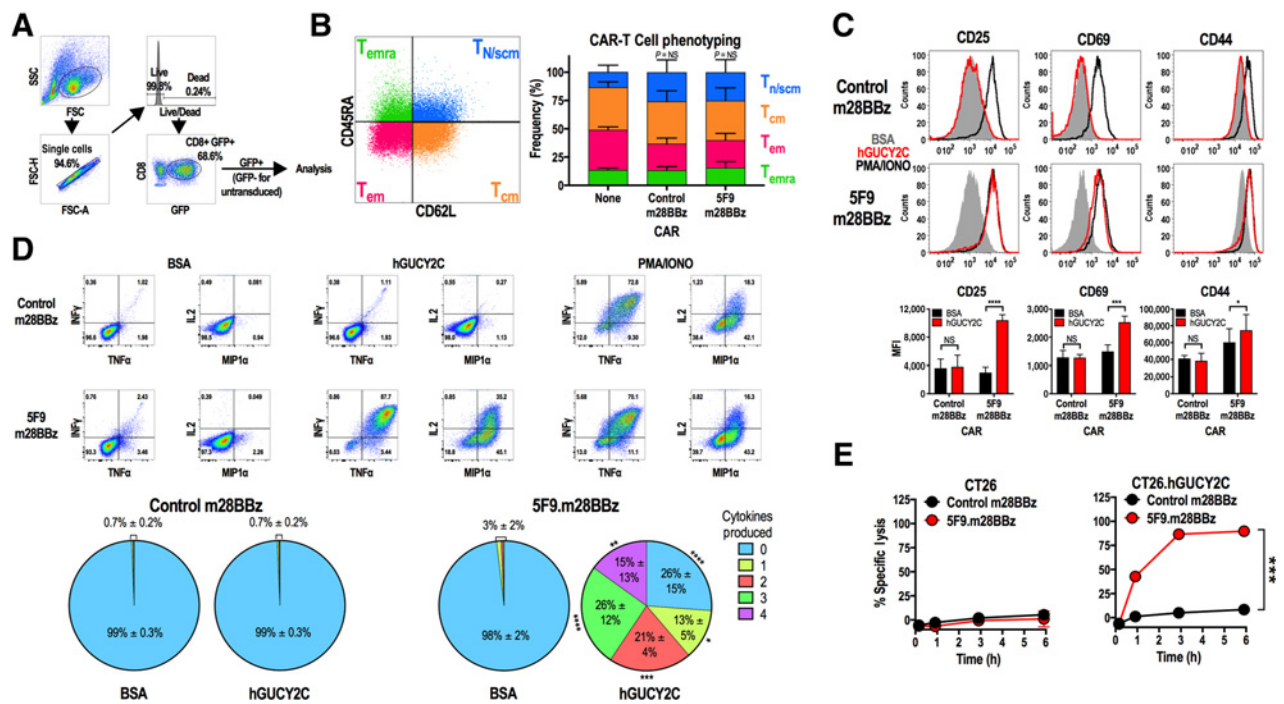


Figure 2. hGUCY2C-specific CARs mediate antigen-dependent T-cell activation and effector functions. **A-E**, Murine CD8⁺ T cells were left non-transduced (none) or transduced with control 1D3.m28BBz or 5F9.m28BBz CAR constructs as indicated. **A**, Gating strategy for all analyses in **B-D**. **B**, Representative CAR-T cell phenotyping plot based on CD45RA and CD62L. Two-way ANOVA; NS: not significant; bars: mean \pm SD from 2 to 3 independent experiments; T_{n/scm}: naive or T memory stem cells; T_{cm}: central memory T cells; T_{em}: effector memory T cells; T_{emra}: effector memory T cells expressing CD45RA. **C** and **D**, 10⁶ CAR-T cells were stimulated for 6 hours with plate-coated antigen (BSA or hGUCY2C) or PMA and ionomycin (PMA/IONO). T-cell activation markers (CD25, CD69, or CD44) and intracellular cytokine production (IFN γ , TNF α , IL2, and MIP1 α) were then quantified by flow cytometry. Graphs indicate the mean \pm SD (**C**) activation marker upregulation (MFI) and (**D**) polyfunctional cytokine production (% of CAR⁺ cells) from 3 independent experiments. **E**, Parental CT26 or CT26.hGUCY2C mouse colorectal cancer cells in an E-Plate were treated with CAR-T cells (5:1 E:T ratio), media, or 2.5% Triton-X 100 (Triton), and the relative electrical impedance was quantified every 15 minutes for 10 hours to quantify cancer cell death (normalized to time = 0). Percent specific lysis values were calculated using impedance values following the addition of media and Triton for normalization (0% and 100% specific lysis, respectively). Two-way ANOVA, **B-E**; *, $P < 0.05$; **, $P < 0.01$; ***, $P < 0.001$; ****, $P < 0.0001$.

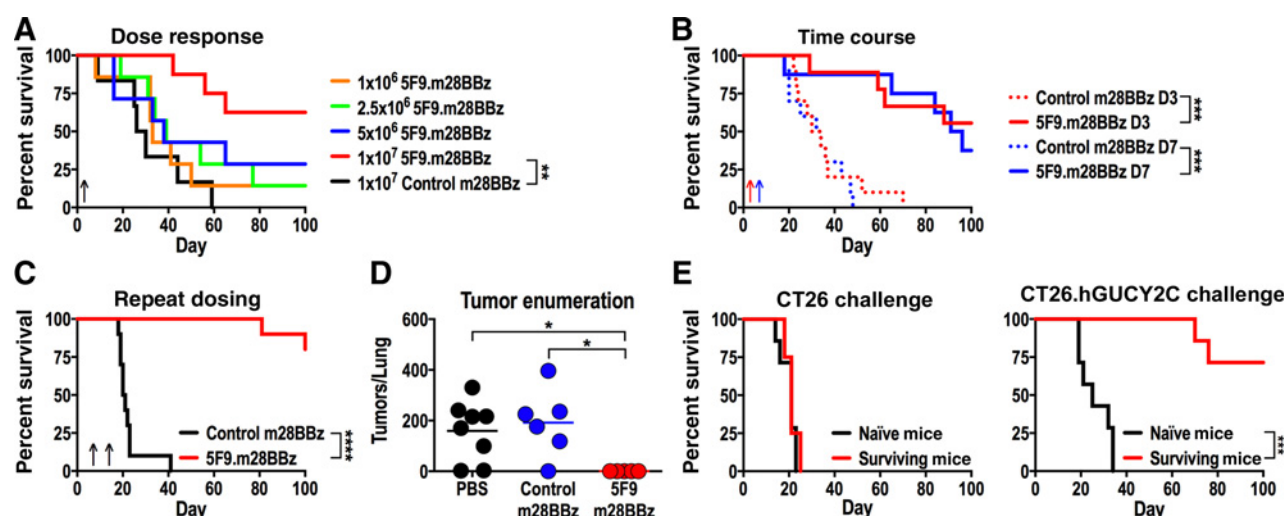


Figure 3. hGUCY2C CAR-T cells provide long-term protection in a syngeneic lung metastasis model. **A–E**, BALB/c mice were injected with 5×10^5 CT26.hGUCY2C cells via the tail vein to establish lung metastases. Control (4D5.m28BBz) or 5F9.m28BBz CAR constructs were transduced into murine CD8⁺ T cells. **A**, Mice were treated 3 days later with 5 Gy total body irradiation (TBI) followed by 10^6 to 10^7 5F9.m28BBz ($N = 7$ – 8 /group) or 10^7 control ($N = 6$) CAR-T cells. **B**, Mice were treated on day 3 (D3) or day 7 (D7) with 5 Gy TBI followed by 10^7 control ($N = 10$ /group) or 5F9.m28BBz ($N = 9$ – 10 /group) CAR-T cells. **C**, Mice were treated on day 7 with 5 Gy TBI followed by 10^7 control ($N = 10$) or 5F9.m28BBz ($N = 12$) CAR-T cells on days 7 and 14. **D**, Mice treated on day 7 with 5 Gy TBI and PBS or 10^7 control or 5F9.m28BBz CAR-T cells were sacrificed on day 18, lungs stained with India ink, and tumors/lung enumerated. One-way ANOVA; *, $P < 0.05$. **E**, Surviving mice from **B** and **C** treated with 5F9.m28BBz CAR-T cells or naïve mice were challenged with 5×10^5 CT26 ($N = 4$ – 7 /group) or CT26.hGUCY2C ($N = 7$ /group) cells (rechallenge occurred 16–40 weeks after initial challenge). Log-rank Mantel-Cox test, **A–C** and **E**; **, $P < 0.01$; ***, $P < 0.001$; ****, $P < 0.0001$. Up arrows indicate CAR-T cell treatment days. Each panel indicates an independent experiment.

or chemotherapies, enhance the efficacy of adoptively transferred T cells by eliminating immunosuppressive cells and reducing competition for homeostatic cytokines, including IL7 and IL15 (25, 26). Here, we utilized an immunocompetent mouse model and a nonmyeloablative dose of 5 Gy total body irradiation (TBI) to mimic clinical treatment regimens. Immunocompetent BALB/c mice received CT26.hGUCY2C cells by tail vein to produce lung metastases, followed 3 days later by TBI and increasing doses of mouse CAR-T cells (Fig. 3A). hGUCY2C-targeted 5F9.m28BBz, but not control, CAR-T cells improved survival of mice at a dose of 10^7 T cells (Fig. 3A). This dose was also effective when administered 7 days after cancer cell inoculation (Fig. 3B), and a second dose administered on day 14 further increased median survival compared with a single dose on day 7 (>150 vs. 93.5 days, $P < 0.05$; Fig. 3C). Lungs collected 18 days after cancer cell inoculation (11 days after treatment) contained tumor nodules, confirming that control mice succumbed to lung metastases while 5F9.m28BBz CAR-T cell treatment eliminated macroscopic tumors (Fig. 3D). To determine if surviving mice exhibited persistent protection against hGUCY2C-expressing tumors, long-term survivors (161–282 days following initial cancer cell inoculation) were challenged with either parental CT26 or CT26.hGUCY2C cells by tail-vein injection to examine hGUCY2C-specific protection (Fig. 3E). CT26 tumors are known to harbor the gp70 envelope protein derived from murine leukemia virus that generates protective gp70-specific CD8⁺ T-cell responses in some vaccination regimens (27). Here, long-term surviving and naïve mice challenged with parental CT26 cancer cells exhibited identical death rates, indicating that long-term survivors did not produce a protective immune response to gp70 or other antigens expressed in CT26 cells (Fig. 3E). Conversely, long-term survi-

vers were protected against CT26.hGUCY2C cancer cells compared with naïve control mice, indicating that 5F9.m28BBz CAR-T cells produce persistent protection against hGUCY2C-expressing tumors (Fig. 3E).

hGUCY2C CAR-T cells recognize human colorectal tumors

We next determined if hGUCY2C CAR-T cells recognized native hGUCY2C on human colorectal tumors. The recombinant hGUCY2C-specific antibody 5F9 stained hGUCY2C on the surface of GUCY2C-expressing T84 (Fig. 4A), but not GUCY2C-deficient SW480 (Supplementary Fig. S9A) human colorectal cancer cells. Correspondingly, 5F9.m28BBz CAR-T cells lysed T84 (Fig. 4B), but not SW480 (Supplementary Fig. S9B) cancer cells *in vitro* in a time-dependent manner. Control CAR-T cells did not kill either human cancer cell type, indicating that killing was antigen-dependent (Fig. 4B; Supplementary Fig. S9B). Human T cells expressing a human 5F9 CAR construct (5F9.h28BBz) produced effector cytokines following GUCY2C stimulation and killed human colorectal cancer cells endogenously expressing hGUCY2C (Supplementary Fig. S10). Mouse T cells expressing hGUCY2C-specific (5F9.m28BBz), but not control, CAR effectively treated T84 human colorectal tumor xenografts in a peritoneal metastases model (Fig. 4C–E). Together, these data indicated that hGUCY2C-specific CAR constructs produced with the 5F9 scFv can redirect T-cell-mediated killing of human colorectal tumors endogenously expressing hGUCY2C.

Adoptive T-cell therapies targeting colorectal tumor antigens have been limited by antigen "on-target, off-tumor" toxicities (4, 5). We previously validated GUCY2C as a potential target for CAR-T cell treatment in a completely syngeneic mouse model in which CARs targeting mouse GUCY2C promoted

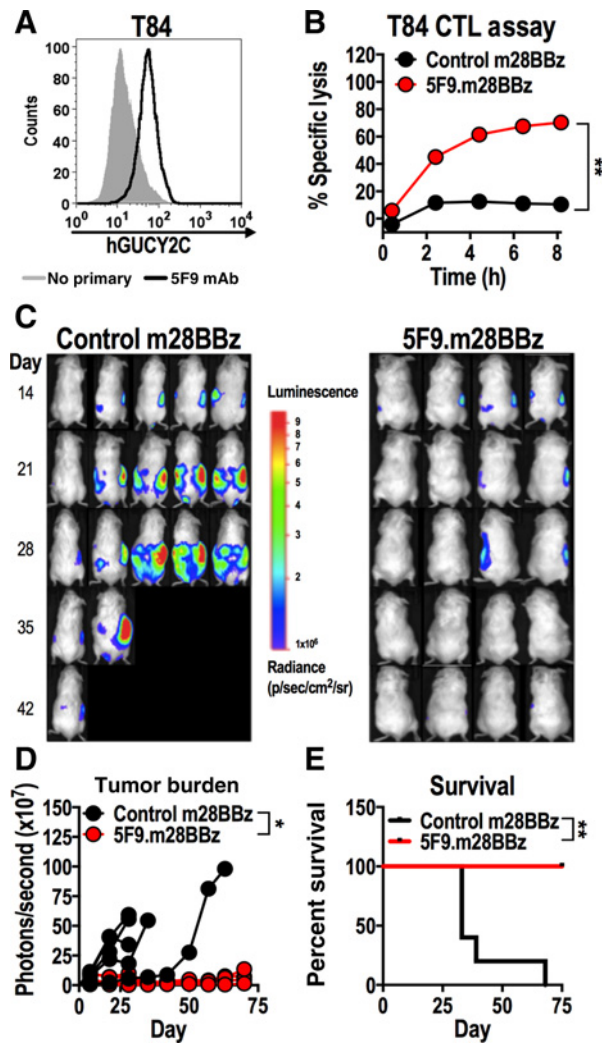


Figure 4. hGUCY2C CAR-T cells eliminate human colorectal tumor xenografts. **A**, hGUCY2C expression on T84 human colorectal cancer cells was quantified by flow cytometry using the recombinant 5F9 antibody. **B–E**, Control (ID3.m28BBz) or 5F9.m28BBz CAR constructs were transduced into murine CD8⁺ T cells. **B**, T84 colorectal cancer cells in an E-Plate were treated in duplicate with 5F9-m28BBz or control CAR-T cells (5:1 E:T ratio), media, or 10% Triton-X 100 (Triton), and the relative electrical impedance was measured every 15 minutes for 20 hours to quantify cancer cell death (normalized to time = 0). Percent specific lysis values were calculated using impedance values following the addition of media and Triton for normalization (0% and 100% specific lysis, respectively). Two-way ANOVA; **, $P < 0.01$; representative of two independent experiments. **C–E**, Immunodeficient NSG mice were injected with 2.5×10^6 luciferase-expressing T84 colorectal cancer cells via intraperitoneal injection and were treated with 10^7 control ($N = 5$ /group) or 5F9-m28BBz ($N = 4$ /group) CAR-T cells on day 14 by intraperitoneal injection. **C** and **D**, Total tumor luminescence (photons/second) was quantified just prior to T-cell injection and weekly thereafter. Two-way ANOVA; *, $P < 0.05$. **E**, Mice were followed for survival. Log-rank Mantel-Cox test; *, $P < 0.05$.

antitumor efficacy in the absence of toxicities to the normal GUCY2C-expressing intestinal epithelium (12). Here, we produced a human GUCY2C-specific CAR from an antibody that is currently used as an antibody–drug conjugate in clinical trials

for GUCY2C-expressing malignancies (NCT02202759 and NCT02202785) and demonstrated its ability to induce T-cell activation, effector function, and antitumor efficacy in both syngeneic and human colorectal tumor xenograft mouse models using murine T cells. CARs produced from the 5F9 scFv do not cross-react with murine GUCY2C (Supplementary Fig. S11), preventing quantification of intestinal toxicity in mouse models. Differences in the antigen-recognition domain of the CAR described here and the murine CAR previously described (12), as well as inherent differences between mice and humans, suggest caution in GUCY2C CAR-T cell administration to humans, despite murine GUCY2C CAR-T cell safety data (12). Thus, appropriate safety measures should be considered when translating the use of GUCY2C CAR-T cells into the clinic, including transient CAR expression by mRNA electroporation (28) or incorporation of suicide genes (29). Nevertheless, GUCY2C-targeted CAR-T cells are an attractive tool for the T-cell therapy armamentarium, a paradigm that is limited by the lack of suitable antigen targets (30).

Disclosure of Potential Conflicts of Interest

M.S. Magee, T.R. Baybutt, and A.E. Snook have ownership interest in U.S. Provisional Patent Application No. 62/643,850. S.A. Waldman is on the board of directors for Targeted Diagnostics & Therapeutics, Inc., reports receiving a commercial research grant from Targeted Diagnostics & Therapeutics, Inc. and Synergy Pharmaceuticals, Inc., has received speakers bureau honoraria from Synergy Pharmaceuticals, Inc., has ownership interest in Thomas Jefferson University, and is a consultant/advisory board member for Targeted Diagnostics & Therapeutics, Inc. No potential conflicts of interest were disclosed by the other authors.

Authors' Contributions

Conception and design: M.S. Magee, T.S. Abraham, N.A. Ridge, S.A. Waldman, A.E. Snook
Development of methodology: M.S. Magee, T.R. Baybutt, N.A. Ridge, G.P. Marszalowicz, A.R. Hersperger, A.E. Snook
Acquisition of data (provided animals, acquired and managed patients, provided facilities, etc.): M.S. Magee, T.R. Baybutt, J.C. Flickinger Jr, N.A. Ridge, G.P. Marszalowicz, P. Prajapati, A.R. Hersperger
Analysis and interpretation of data (e.g., statistical analysis, biostatistics, computational analysis): M.S. Magee, T.S. Abraham, T.R. Baybutt, J.C. Flickinger Jr, N.A. Ridge, S.A. Waldman, A.E. Snook
Writing, review, and/or revision of the manuscript: M.S. Magee, T.S. Abraham, G.P. Marszalowicz, S.A. Waldman, A.E. Snook
Administrative, technical, or material support (i.e., reporting or organizing data, constructing databases): T.S. Abraham, N.A. Ridge
Study supervision: T.S. Abraham, S.A. Waldman, A.E. Snook

Acknowledgments

Financial support was provided by NIH (P30 CA56036, R01 CA204881, and R01 CA206026 to S.A. Waldman; F31 CA171672 to M.S. Magee), Targeted Diagnostic & Therapeutics, Inc. (to S.A. Waldman), Courtney Ann Diacont Memorial Foundation (to S.A. Waldman), PhRMA Foundation (to A.E. Snook), the W.W. Smith Charitable Trust (to A.E. Snook), and Margaret Q. Landenberger Research Foundation (to A.E. Snook). S.A. Waldman is the Samuel M.V. Hamilton Professor of Medicine of Thomas Jefferson University. This project was funded, in part, by grants from the Pennsylvania Department of Health (SAP #4100059197, SAP #4100051723 to S.A. Waldman). The Department specifically disclaims responsibility for any analyses, interpretations, or conclusions. The funders had no role in study design, data collection and analysis, decision to publish, or preparation of the manuscript.

Received December 7, 2016; revised November 3, 2017; accepted March 22, 2018; published first April 3, 2018.

References

1. Maude SL, Frey N, Shaw PA, Aplenc R, Barrett DM, Bunin NJ, et al. Chimeric antigen receptor T cells for sustained remissions in leukemia. *N Engl J Med* 2014;371:1507–17.
2. Lee DW, Kochenderfer JN, Stetler-Stevenson M, Cui YK, Delbrook C, Feldman SA, et al. T cells expressing CD19 chimeric antigen receptors for acute lymphoblastic leukaemia in children and young adults: a phase 1 dose-escalation trial. *Lancet* 2015;385:517–28.
3. Louis CU, Savoldo B, Dotti G, Pule M, Yvon E, Myers GD, et al. Antitumor activity and long-term fate of chimeric antigen receptor-positive T cells in patients with neuroblastoma. *Blood* 2011;118:6050–6.
4. Parkhurst MR, Yang JC, Langan RC, Dudley ME, Nathan DA, Feldman SA, et al. T cells targeting carcinoembryonic antigen can mediate regression of metastatic colorectal cancer but induce severe transient colitis. *Mol Ther* 2011;19:620–6.
5. Morgan RA, Yang JC, Kitano M, Dudley ME, Laurencot CM, Rosenberg SA. Case report of a serious adverse event following the administration of T cells transduced with a chimeric antigen receptor recognizing ERBB2. *Mol Ther* 2010;18:843–51.
6. Aka AA, Rappaport JA, Pattison AM, Sato T, Snook AE, Waldman SA. Guanylate cyclase C as a target for prevention, detection, and therapy in colorectal cancer. *Expert Rev Clin Pharmacol* 2017;10:549–57.
7. Valentino MA, Lin JE, Snook AE, Li P, Kim GW, Marszalowicz G, et al. A uroguanylin-GUCY2C endocrine axis regulates feeding in mice. *J Clin Invest* 2011;121:3578–88.
8. Carrithers SL, Barber MT, Biswas S, Parkinson SJ, Park PK, Goldstein SD, et al. Guanylyl cyclase C is a selective marker for metastatic colorectal tumors in human extraintestinal tissues. *Proc Natl Acad Sci USA* 1996;93:14827–32.
9. Birbe R, Palazzo JP, Walters R, Weinberg D, Schulz S, Waldman SA. Guanylyl cyclase C is a marker of intestinal metaplasia, dysplasia, and adenocarcinoma of the gastrointestinal tract. *Hum Pathol* 2005;36:170–9.
10. Wolfe HR, Mendizabal M, Lleong E, Cuthbertson A, Desai V, Pullan S, et al. In vivo imaging of human colon cancer xenografts in immunodeficient mice using a guanylyl cyclase C-specific ligand. *J Nucl Med* 2002;43:392–9.
11. Coradini D, Casarsa C, Oriana S. Epithelial cell polarity and tumorigenesis: new perspectives for cancer detection and treatment. *Acta Pharmacol Sin* 2011;32:552–64.
12. Magee MS, Kraft CL, Abraham TS, Baybutt TR, Marszalowicz GP, Li P, et al. GUCY2C-directed CAR-T cells oppose colorectal cancer metastases without autoimmunity. *Oncoimmunology* 2016;5:e1227897.
13. Marszalowicz GP, Snook AE, Magee MS, Merlino D, Berman-Booty LD, Waldman SA. GUCY2C lysosomotropic endocytosis delivers immunotoxin therapy to metastatic colorectal cancer. *Oncotarget* 2014;5:9460–71.
14. Snook AE, Li P, Stafford BJ, Faul EJ, Huang L, Birbe RC, et al. Lineage-specific T-cell responses to cancer mucosa antigen oppose systemic metastases without mucosal inflammatory disease. *Cancer Res* 2009;69:3537–44.
15. Snook AE, Magee MS, Schulz S, Waldman SA. Selective antigen-specific CD4(+) T-cell, but not CD8(+) T- or B-cell, tolerance corrupts cancer immunotherapy. *Eur J Immunol* 2014;44:1956–66.
16. Hodson CA, Ambrogi IG, Scott RO, Mohler PJ, Milgram SL. Polarized apical sorting of guanylyl cyclase C is specified by a cytosolic signal. *Traffic* 2006;7:456–64.
17. Charney AN, Egnor RW, Alexander-Chacko JT, Zaharia V, Mann EA, Giannella RA. Effect of *E. coli* heat-stable enterotoxin on colonic transport in guanylyl cyclase C receptor-deficient mice. *Am J Physiol Gastrointest Liver Physiol* 2001;280:G216–21.
18. Kuhn M, Adermann K, Jahne J, Forssmann WG, Rechkemmer G. Segmental differences in the effects of guanylin and *Escherichia coli* heat-stable enterotoxin on Cl⁻ secretion in human gut. *J Physiol* 1994;479:433–40.
19. Guarino A, Cohen MB, Overmann G, Thompson MR, Giannella RA. Binding of *E. coli* heat-stable enterotoxin to rat intestinal brush borders and to basolateral membranes. *Dig Dis Sci* 1987;32:1017–26.
20. Witek ME, Nielsen K, Walters R, Hyslop T, Palazzo J, Schulz S, et al. The putative tumor suppressor Cdx2 is overexpressed by human colorectal adenocarcinomas. *Clin Cancer Res* 2005;11:8549–56.
21. Liu X, Jiang S, Fang C, Yang S, Olalere D, Pequignot EC, et al. Affinity-tuned ErbB2 or EGFR chimeric antigen receptor T cells exhibit an increased therapeutic index against tumors in mice. *Cancer Res* 2015;75:3596–607.
22. Mule JJ, Shu S, Schwarz SL, Rosenberg SA. Adoptive immunotherapy of established pulmonary metastases with LAK cells and recombinant interleukin-2. *Science* 1984;225:1487–9.
23. Shultz LD, Lyons BL, Burzenski LM, Gott B, Chen X, Chaleff S, et al. Human lymphoid and myeloid cell development in NOD/LtSz-scid IL2R gamma null mice engrafted with mobilized human hemopoietic stem cells. *J Immunol* 2005;174:6477–89.
24. Xu XJ, Song DG, Poussin M, Ye Q, Sharma P, Rodriguez-Garcia A, et al. Multiparameter comparative analysis reveals differential impacts of various cytokines on CART cell phenotype and function ex vivo and in vivo. *Oncotarget* 2016;7:82354–68.
25. Muranski P, Boni A, Wrzesinski C, Citrin DE, Rosenberg SA, Childs R, et al. Increased intensity lymphodepletion and adoptive immunotherapy—how far can we go? *Nat Clin Pract Oncol* 2006;3:668–81.
26. Gattinoni L, Finkelstein SE, Klebanoff CA, Antony PA, Palmer DC, Spiess PJ, et al. Removal of homeostatic cytokine sinks by lymphodepletion enhances the efficacy of adoptively transferred tumor-specific CD8⁺ T cells. *J Exp Med* 2005;202:907–12.
27. Huang AY, Gulden PH, Woods AS, Thomas MC, Tong CD, Wang W, et al. The immunodominant major histocompatibility complex class I-restricted antigen of a murine colon tumor derives from an endogenous retroviral gene product. *Proc Natl Acad Sci U S A* 1996;93:9730–5.
28. Beatty GL, Haas AR, Maus MV, Torigian DA, Soulen MC, Plesa G, et al. Mesothelin-specific chimeric antigen receptor mRNA-engineered T cells induce anti-tumor activity in solid malignancies. *Cancer Immunol Res* 2014;2:112–20.
29. Casucci M, Bondanza A. Suicide gene therapy to increase the safety of chimeric antigen receptor-redirected T lymphocytes. *J Cancer* 2011;2:378–82.
30. Rosenberg SA. Decade in review-cancer immunotherapy: Entering the mainstream of cancer treatment. *Nat Rev Clin Oncol* 2014;11:630–2.